MODELING PERIPHERAL VISIBILITY UNDER HEADLAMP ILLUMINATION

Transportation Research Board 16th Biennial Symposium on Visibility and Simulation
Iowa City, IA, June 2-4, 2002

John D. Bullough
Lighting Research Center, Rensselaer Polytechnic Institute
21 Union Street
Troy, NY 12180 USA
Email: bulloj@rpi.edu
Tel: (518) 687-7100
Fax: (518) 687-7120

ABSTRACT
Undoubtedly, the detection of peripheral objects and pedestrians while driving is an important visual task. However, there are few data that describe the impact of parameters such as headlamp illumination, peripheral angle and target reflectance upon the speed and accuracy with which one can detect peripheral targets. The present paper outlines a framework for the development of a model that predicts reaction times and detection percentages to small targets of varying reflectance, and located at various positions in the field of view. The preliminary model closely matches data from independently-performed field studies using halogen and high intensity discharge headlamp sets having illumination characteristics that conform to North American and European requirements for headlamp beam patterns. The modeling approach discussed in the paper allows characteristics such as the effective field of view to be described. Further, the approach could be extended to incorporate driver age, target size, visual clutter, spectral power distribution, glare and ambient roadway illumination into the model predictions. Such a model could serve as a useful complement to existing models of on-axis (foveal) visual performance in driving contexts.

INTRODUCTION

Data describing reaction times and detection percentages to peripheral small targets of varying reflectance are used to develop a preliminary model of peripheral visibility under headlamp illumination that could be used in subsequent studies of headlamp beam effectiveness.

EXPERIMENTAL METHODS

The data used to develop the model were collected during two separate experiments (see Figure 1).[1,2] Subjects (ranging in age from under 30 to over 50 years in each experiment; all subjects reported having normal vision and possessed drivers licenses, but were not formally screened for vision) sat in the driver's seat of a passenger automobile, in front of which was mounted one of several sets of properly aimed headlamps that provided forward illumination. The automobile was located along an unused airport runway with no electric lighting. Six small square (20 cm in length) targets were positioned on the ground 60 m in front of the vehicle at 5^{o} intervals, between 7.5^{o} from the left of the centerline and 17.5^{o} to the right of the centerline. Ambient lighting from moonlight (the experiment was never run during a full moon nor during a new moon) provided 0.1-0.2 lx on the targets. The targets subtended a solid angle (ω) of 1.2×10^{-5} sr at subjects' eyes. Targets consisted of arrays of flip dots used in variable message signs; the flip dot disks were black on one side and white on another. When the flip dots were switched to the white side, the average reflectance (ρ) of the target surface was 0.4. While subjects were in the automobile, they performed a simple tracking task displayed using light emitting diodes that was positioned along the centerline in front of the vehicle in order to ensure that their direction of view remained constant.

During the experiment, subjects held a control box containing a knob for the tracking task and a button for the response to the targets. Subjects held down the button while performing the tracking task and released it when they detected the transition of a flip dot target from black (its usual state) to white. Targets were presented at random intervals ranging from 3 to 5 seconds, and at random angles for each experimental session. Using a microcomputer controller in the control box, the time taken to detect the onset of the target could be measured and relayed to a personal computer for data storage. If no response was recorded within 1 second, that particular trial was considered a "missed target" and a reaction time of 1000 ms was relayed to the computer (missed target data were not incorporated into the reaction time model). A reduced-contrast target was created using the same flip-dot target, but placing in front of it a neutral filter, positioned so as not to reflect headlamp illumination back toward the subject's location; the resulting target had a reduced reflectance (ρ) of 0.2.

As stated above, data were collected during two separate experiments, one using two sets of halogen and one set of high intensity discharge (HID) headlamps conforming to European beam pattern standards, and one using one set each of halogen and HID headlamps meeting North American standards. In general, the HID headlamps produced more illumination at peripheral angles than the halogen headlamps for both beam pattern types. All systems produced higher illuminances on the targets than were provided by ambient conditions. The vertical illuminance on each target was measured during each experiment and for each type of headlamp system.

Twelve subjects participated in each experiment, conducted over several night sessions in groups of three or four subjects during summer 2000 and summer 2001. Each subject completed four reaction time trials to each target position and reflectance under each headlamp system. As will be seen below, despite the fact that each experiment used a different set of twelve subjects, the mean reaction times and detection percentages for a given angle and target illuminance were very consistent between the two groups, so that the data from the two experiments could be combined into a single data set. The illuminance on the targets was not originally treated as an independent variable.[1,2] However, the variations in headlamp system output, from low to relatively high, exhibited fairly continuous ranges, making it convenient to study this variable as if it were an independent variable for the purpose of this paper.

The data points in Figures 2 through 5 show the mean reaction times, and in Figures 6 through 9 show the detection percentages, for each peripheral angle (θ), reflectance (ρ) and illuminance (E). Each point represents the mean of up to 48 individual trials (as described above, fewer than 48 reaction time trials are used when misses occurred; when a target was never detected, there is no corresponding data point in the reaction time graphs). For clarity, standard deviations for the reaction time data (typically between 50 and 100 ms) are not shown in Figures 2 through 5; refer to Van Derlofske *et al.*[1,2] for further details. Because five headlamp systems were used at each position, each graph should contain up to five data points for each target reflectance; since the visual angles were the same, data for the targets at 2.5^{o} and 7.5^{o} to the left of the centerline were plotted on the same graphs as data for the 2.5^{o} and 7.5^{o} targets to the right of the centerline, respectively. As would be expected, the illuminances at 2.5^{o} and 7.5^{o} were higher on the passenger side than on the driver side.

He *et al.*[3] demonstrated that light sources with higher short-wavelength or scotopic, output result in shorter peripheral response times. Thus, because the HID headlamps used in the experiments have a slightly higher (<10%) scotopic output than the halogen lamps, they would be expected to result in shorter reaction times. Such spectral differences between the halogen and HID lamps are not considered in the present model, however, although subsequent iterations of it could certainly incorporate data on headlamp spectrum and peripheral visual performance.

DEVELOPMENT OF PREDICTIVE MODEL FOR PERIPHERAL REACTION TIMES

Visual reaction times have been modeled closely by functions having the form:[3]

$$RT = aL^{-0.33} + n \qquad (1)$$

where RT is the reaction time (in ms);
a is a function of target size, reflectance and location;
L is the luminance of the target (in cd/m^2);
and n is a constant time (in ms) corresponding to the time for nonvisual responses such as motor responses associated with releasing a control switch, and is dependent upon the age of a set of subjects and the specific experimental protocol.

As described above, the value of a depends upon factors such as the size of the target, its reflectance and its location in the field of view, and a should be properly notated $a_{\omega,\rho,\theta}$ (for clarity, the simpler notation a is used). However, because the target size ω was fixed in the experiments described above (at 1.2×10^{-5} sr), a will only be considered henceforth only as a function of target reflectance ρ and viewing angle θ.

The exponent in Equation 1 was found in several previous reaction time experiments[3-5] to have a value close to -0.33 and was therefore fixed at this value. In the experiments described above, the luminance L of the target is proportional to the illuminance E on the target (for a given reflectance). Since the target's reflectance ρ determines its contrast against the background, and since only the illuminance from the headlamp is itself a function of the headlamp's performance, the predictive model outlined below uses headlamp illuminance E as a parameter, rather than target luminance L.

The reaction time data plotted in Figures 2 through 5, for targets having each value of ρ (0.4 or 0.2) and off-axis angle (θ, either 2.5^{o}, 7.5^{o}, 12.5^{o} or 17.5^{o}) were therefore fitted to functions having the form:

$$RT = aE^{-0.33} + n \quad (2)$$

where a is a parameter that is a function of target reflectance and position;
E is the illuminance on the target (in lx);
and n is the nonvisual response time (in ms).

The data were fit to this form using different values for n ranging from 200 ms, the probable minimum for a visual response time,[3] to 450 ms, which was close to the shortest reaction time measured in either experiment, in 50-ms intervals. The coefficients of correlation (r^2) for these fits were highest when n had a value of 400 ms; this value for n was therefore subsequently used in developing the model. This value corresponds to the specific experimental conditions, where subjects released a switch held by their fingers; if the response had been to press or release a foot pedal, for example, n would likely have been larger. Table 1 shows the values of a for each value of ρ and θ, as well as the values of r^2 for the fitted functions. Figure 10 shows these values of a plotted against θ for each value of ρ.

The values of a in Table 1 are higher when ρ is 0.2, than when it is 0.4, which is as expected since reaction times are longer to a target of lower reflectance. The values of a also show similar trends for each target reflectance ρ: there is less variation between 2.5° and 7.5° and between 12.5° and 17.5°, than there is between 7.5° and 12.5°. There appears to be an angular region between 7.5° and 12.5° for both target reflectances, where reaction times to peripheral targets increase quite rapidly. (See the Discussion section for a description of other visual phenomena following this pattern.)

In order to predict the value of a, a secondary function was used, having the form:

$$a = b - (b - c)/(1 + (\theta/d)^e) \quad (3)$$

where θ is the peripheral angle of the target (in degrees);
a is as defined in Equation 2;
b is the maximum value of a for a given reflectance ρ;
c is the minimum value of a for a given reflectance ρ;
d is the angle θ at which the greatest change in a occurs (in degrees);
and e is the relative slope of the function represented by a.

In this function, the expression (b - c) is the range of allowable values for a. Fitting Equation 3 to the values of a in Table 1 led to the values of b, c and d shown in Table 2. The value of e for all fits was set to 8, in order to visually match the slopes of the trend lines in Figure 10.

In order to estimate the values of b, c and d as a function of the target reflectance ρ, these values were fitted to power functions having a form as in Equation 4:

$$b, c \text{ or } d = x\rho^y \quad (4)$$

where ρ is the target reflectance;
and b, c and d are as defined in Equation 3.

The logic behind using power functions is that at very low reflectance, the targets will be close to minimally visible, and the corresponding response times to that target should approach infinity. At higher reflectances, reaction times would decrease but with diminishing returns. But because the fits below are based on a sample of only two reflectances, subsequent refinements of the model should probe the effect of target reflectance further. As preliminary estimates, however, the power fits shown below predict what would intuitively be expected as reflectance were changed from very low to high values. The parameter b was closely predicted by the function (Figure 11):

$$b = 206\rho^{-0.22} \quad (4a)$$

and d by the function (Figure 12):

$$d = 11\rho^{0.18} \quad (4b)$$

It was further observed that the range *(b - c)* was similar for each reflectance; therefore, a constant intermediate value of 76 for *(b - c)* was used, so that *c* had a value of:

$$c = 206\rho^{-0.22} - 76 \quad (4c)$$

Using these values for *b*, *c* and *d*, and using 8 as the value for *e* gives the following prediction for *a*:

$$a = 206\rho^{-0.22} - 76/[1 + (\theta/11\rho^{0.18})^8] \quad (5)$$

The solid (for $\rho = 0.4$) and dashed (for $\rho = 0.2$) curves in Figure 10 show the resulting predictions for *a*. Substituting these values of *a* into Equation 2 (and using n = 400 ms) gives predictions having the form of the solid (for $\rho = 0.4$) and dashed (for $\rho = 0.2$) curves in Figures 2 through 5. Table 3 gives the resulting coefficients of correlation (r^2) when the predicted reaction times were compared with the actual reaction times shown in these figures. Rearranging terms, the reaction time model can be simplified to:

$$RT = [A\rho^{-0.22} - B(C\theta^8\rho^{-1.44} + 1)^{-1}]E^{-0.33} + 400 \quad (6)$$

where $A = 206$;
$B = 76$;
$C = 3.55 \times 10^{-7}$;
and *RT*, *E*, θ and ρ are as defined in Equations 1 through 4.

DEVELOPMENT OF PREDICTIVE MODEL FOR PERIPHERAL TARGET DETECTION

A similar approach was taken for the peripheral target detection model, using illuminance from the headlamp rather than target luminance in order to keep the characteristics of the headlamp separate from those of the target. Additionally, as a single target size was used, the resulting model only considers the target's reflectance and position. Upon inspection of the data plotted in Figures 6 through 9, the data appear to follow an asymptotic form, with a high proportion of missed targets at low illuminances, approaching zero at high illuminances. A power function was therefore used to model this characteristic of the missed target data (*MT*) in Figures 6 through 9:

$$MT = fE^{-g} \text{ (or 1 when } fE^{-g} > 1) \quad (7)$$

where *MT* is the proportion of missed targets;
and *f* and *g* are parameters that are a function of target reflectance and position.

Since the proportion of missed targets can never exceed 1, the function is modified as described in Equation 7 to have a maximum value of 1, so that the illuminance at which the term $fE^{-g} = 1$ could be thought of as a threshold detection illuminance. The best fitting values of *f* and *g*, and the coefficients of correlation (r^2) for each value of ρ and θ are shown in Table 4 and plotted in Figures 13 and 14.

The points in Figure 13 show very similar trends as those for parameter *a* shown in Figure 10, having an asymptotic shape that can be represented by the form:

$$f = h - (h - j)/(1 + (\theta/k)^m) \quad (8)$$

where θ is the peripheral angle of the target (in degrees);
f is as defined in Equation 7;
h is the maximum value of *f* for a given reflectance ρ;
j is the minimum value of *f* for a given reflectance ρ;
k is the angle θ at which the greatest change in *f* occurs (in degrees);
and *m* is the relative slope of the function represented by *f*.

Fitting this equation to the values of *f* in Table 4 led to the values of *h*, *j* and *k* shown in Table 5, with a value of *m* set to 8 in order to visually match the slopes in Figure 13. In order to predict these parameters as a function of target reflectance ρ, they were fitted to power functions of the form:

$$h, j \text{ or } k = x\rho^{y} \quad (9)$$

where ρ is the target reflectance;
and *h*, *j* and *k* are as defined in Equation 8.

The parameters *h* and *k*, as might be expected, behave similarly to *b* and *d* in Equations 4a and 4b (Figures 15 and 16).

$$h = 0.68\rho^{-0.2} \quad (9a)$$

$$k = 17\rho^{0.29} \quad (9b)$$

Further, much as with the value of (*b* - *c*) in Equation 3, the term (*h* - *j*) appeared to have a constant value of approximately 0.68, so *j* was not modeled except as an offset from *h*:

$$j = 0.68\rho^{-0.2} - 0.68 \quad (9c)$$

Using these values of *h*, *j* and *k* (and assigning a value of 8 to *m*) gives the following prediction for *f*:

$$f = 0.68\rho^{-0.2} - 0.68/[1 + (\theta/17\rho^{0.29})^{8}] \quad (10)$$

The curves in Figure 13 show these predictions alongside the best-fitting values of *f*. As for the parameter *g*, Figure 14 shows that there appears to be a downward trend in *g* as the target's peripheral angle increases, but the data show no clear effect of the target reflectance. As a first approximation, therefore, *g* was fitted to a power function of the peripheral angle θ:

$$g = 1.7\theta^{-0.7} \quad (11)$$

Rearranging the terms in Equations 10 and 11 gives the resulting simplified model for the proportion of missed targets:

$$MT = A[\rho^{-0.2} - (B\theta^{8}\rho^{-2.32} + 1)^{-1}]E^{-1.7\theta^{-0.7}} \quad (12)$$

where $A = 0.68$;
$B = 1.43 \times 10^{-10}$;
and *MT*, *E*, θ and ρ are as defined in Equations 7 through 9.

Table 6 shows the goodness of fit to the observed missed target data, and the curves in Figures 6 through 9 show the model predictions alongside the observed data.

DISCUSSION

The present paper provides a framework for development of a model of peripheral visibility under headlamp illumination. Such predictions could be useful in future studies of optimal beam patterns for drivers to ensure acceptable levels of peripheral visibility. Of interest, the parameter *d* in Equations 3 and 4b, and the parameter *k* in Equations 8 and 9b, correspond to the angles at which the visual response will have begun to worsen significantly. This parameter is perhaps analogous to the effective size of the field of view for a given target reflectance. As reflectance is reduced, this size would also be expected to be reduced, as the present model predicts (see Figures 17 and 18). Similar phenomena, where responses are relatively constant for small visual angles, worsen sharply within a range of angles and then are asymptotic beyond a given angle have been reported for visual inspection tasks, with small or low-contrast tasks having smaller effective visual field sizes or "lobes."[6] Lingard and Rea[7] noted similar trends in their study of responses to self-luminous, peripheral targets of varying contrast and under different spectral

power distributions. Smith and Dimmick[8] also found that visual senstivity seemed to level off rather than worsen monotonically as a function of visual angle during dark adaptation. Of course, other factors that could influence the effective visual field include attention, visual clutter, secondary task dificulty and age.[9]

It should go without saying that further validation work is needed to ensure that the model applies to target reflectances and angles other than those used to derive it. Similarly, target size and headlamp spectrum are other important determinants of peripheral visibility. Still, the fact that two independently conducted experiments[1,2] have been used to derive the preliminary model presented in this paper, bodes well for its refinement and its potential for application in future studies of forward visibility as a function of headlamp beam patterns.

ACKNOWLEDGMENTS

Mark Rea and John Van Derlofske of the Lighting Research Center (LRC) at Rensselaer Polytechnic Institute are gratefully acknowledged for their helpful comments and suggestions. The experimental work on which the models described in this paper are based was conducted by the LRC with support from Philips Automotive Lighting.

REFERENCES

1. Van Derlofske J., J. D. Bullough, and C. M. Hunter. Evaluation of High-Intensity Discharge Automotive Forward Lighting. In *Lighting Technology Developments for Automobiles*, SAE, Warrendale, Pa., 2001, pp. 1-7.
2. Van Derlofske J., J. D. Bullough, and C. M. Hunter. Visual Benefits of High-Intensity Discharge Automotive Forward Lighting. In *Advanced Lighting Technology for Vehicles*, SAE, Warrendale, Pa., 2002, pp. 51-56.
3. He, Y., M. S. Rea, A. Bierman, and J. Bullough. Evaluating Light Source Efficacy Under Mesopic Conditions Using Reaction Times. *Journal of the Illuminating Engineering Society*, Vol. 26, No. 1, 1997, pp. 125-138.
4. Vaughan, P. G., L. D. Costa, and L. Gilden. The Functional Relation of Visual Evoked Response and Reaction Time to Stimulus Intensity. *Vision Research*, Vol. 6, 1966, pp. 645-656.
5. Bullough, J. D., P. R. Boyce, A. Bierman, K. M. Conway, K. Huang, C. P. O'Rourke, C. M. Hunter, and A. Nakata. Response to Simulated Traffic Signals Using Light-Emitting Diode and Incandescent Sources. In *Transportation Research Record 1724*, TRB, National Research Council, Washington, D.C., 2000, pp. 39-46.
6. Boyce, P. R. Visual Inspection. In *Human Factors in Lighting*, Macmillan, New York, N.Y., 1981, pp. 147-169.
7. Lingard, R., and M. S. Rea. Off-Axis Detection at Mesopic Light Levels in a Driving Context. *Journal of the Illuminating Engineering Society*, Vol. 31, No. 1, 2002, pp. 33-39.
8. Smith, J. A., and F. L. Dimmick. The Parameters of Scotopic Sensitivity: 1. The Effect of Size. *Medical Research Laboratory Report Number 174*, Vol. 10, 1951, pp. 56-75.
9. Wolf, E. Studies on the Shrinkage of the Visual Field with Age. In *Highway Research Record 164*, HRB, National Research Council, Washington, D.C., 1967, pp. 1-7.

TABLE 1 Best Fitting Values of *a* for Each Peripheral Angle and Reflectance

Angle, θ	Reflectance, ρ	*a*	r^2
2.5°	0.4	168	0.26
7.5°	0.4	173	0.75
12.5°	0.4	252	0.99
17.5°	0.4	245	0.96
2.5°	0.2	230	0.78
7.5°	0.2	250	0.70
12.5°	0.2	289	0.56
17.5°	0.2	297	0.58

TABLE 2 Best Fitting Values of *b*, *c* and *d* for Each Reflectance

Reflectance, ρ	*b*	*c*	*d*	r^2
0.4	252	165	9.4	0.98
0.2	294	230	8.3	0.99

TABLE 3 Coefficients of Correlation Between Actual and Predicted Reaction Times for Each Target Reflectance and Position

Angle, θ	Reflectance, ρ	r^2
2.5°	0.4	0.35
7.5°	0.4	0.75
12.5°	0.4	0.99
17.5°	0.4	0.97
2.5°	0.2	0.79
7.5°	0.2	0.74
12.5°	0.2	0.58
17.5°	0.2	0.70

TABLE 4 Best Fitting Values of *f* and *g* for Each Peripheral Angle and Reflectance

Angle, θ	Reflectance, ρ	*f*	*g*	r^2
2.5°	0.4	0.18	0.98	0.05
7.5°	0.4	0.10	0.30	0.18
12.5°	0.4	0.43	0.38	0.87
17.5°	0.4	0.76	0.22	0.54
2.5°	0.2	0.26	0.48	0.34
7.5°	0.2	0.31	0.77	0.50
12.5°	0.2	0.80	0.45	0.95
17.5°	0.2	0.93	0.06	0.78

TABLE 5 Best Fitting Values of *h, j* and *k* for Each Reflectance

Reflectance, ρ	*h*	*j*	*k*	r^2
0.4	0.82	0.14	13.0	0.99
0.2	0.94	0.27	10.6	0.99

TABLE 6 Coefficients of Correlation Between Actual and Predicted Missed Target Percentages for Each Target Reflectance and Position

Angle, θ	Reflectance, ρ	r^2
2.5°	0.4	0.01
7.5°	0.4	0.23
12.5°	0.4	0.82
17.5°	0.4	0.57
2.5°	0.2	0.75
7.5°	0.2	0.74
12.5°	0.2	0.96
17.5°	0.2	0.79

FIGURE 1 Experimental apparatus for the target detection experiments.[1,2]

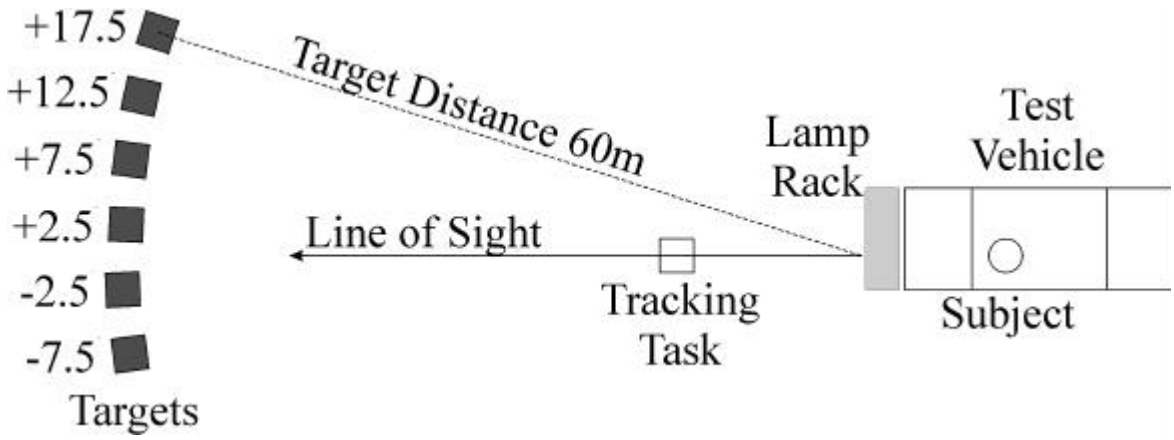

FIGURE 2 Reaction times to targets located 2.5° from the line of sight.

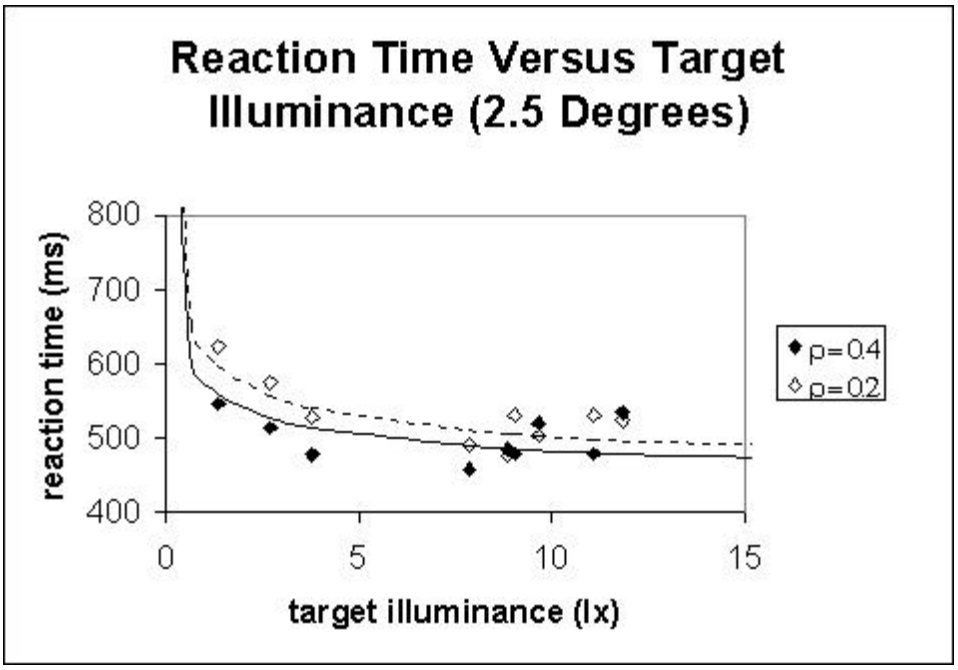

FIGURE 3 Reaction times to targets located 7.5° from the line of sight.

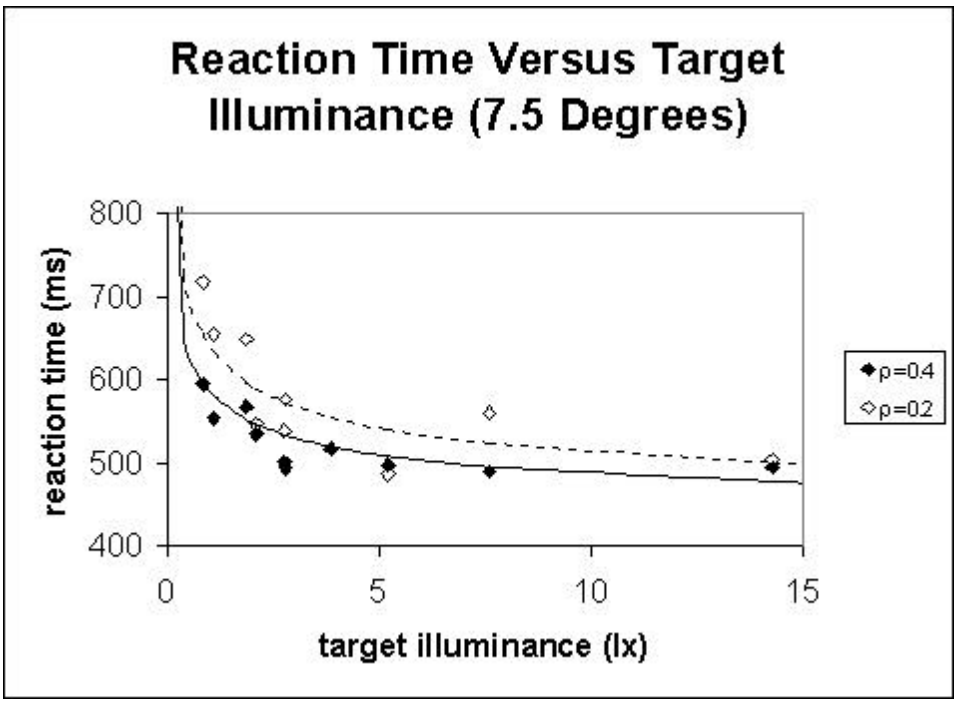

FIGURE 4 Reaction times to targets located 12.5° from the line of sight.

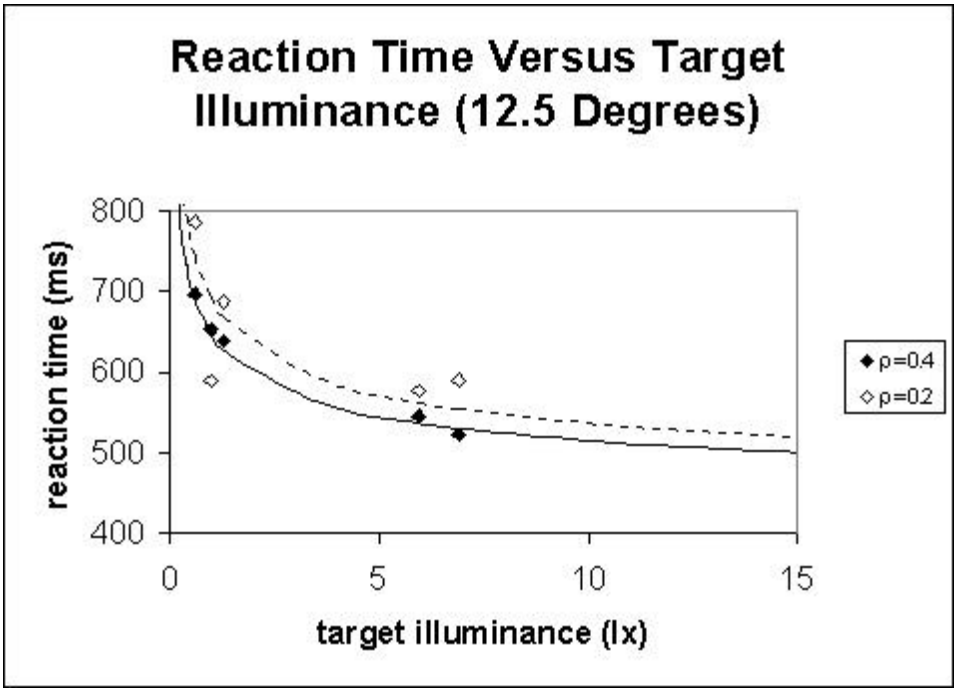

FIGURE 5 Reaction times to targets located 17.5° from the line of sight.

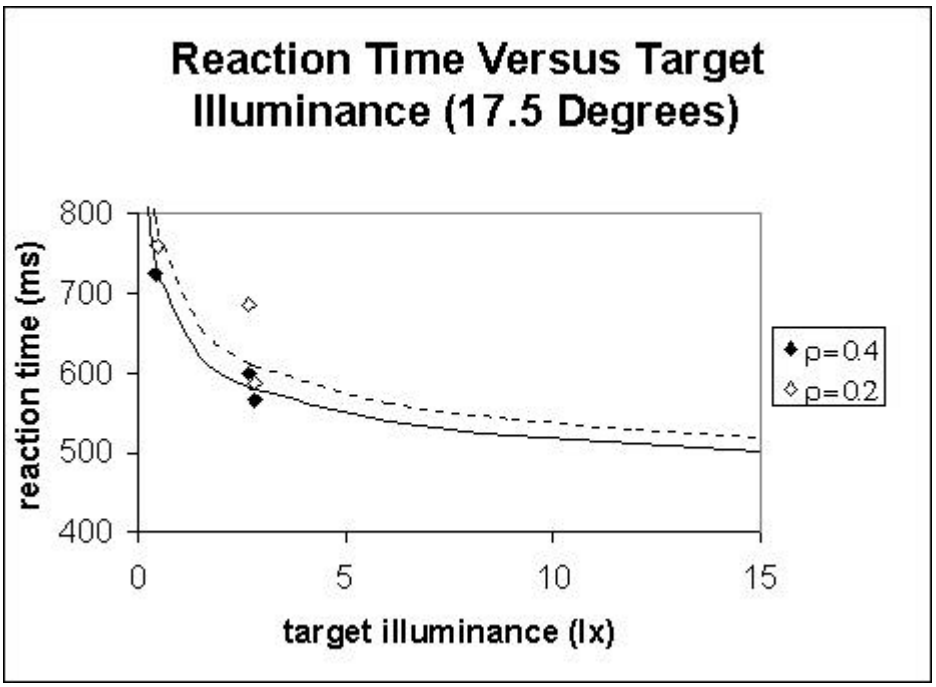

FIGURE 6 Detection percentages for targets located 2.5° from the line of sight.

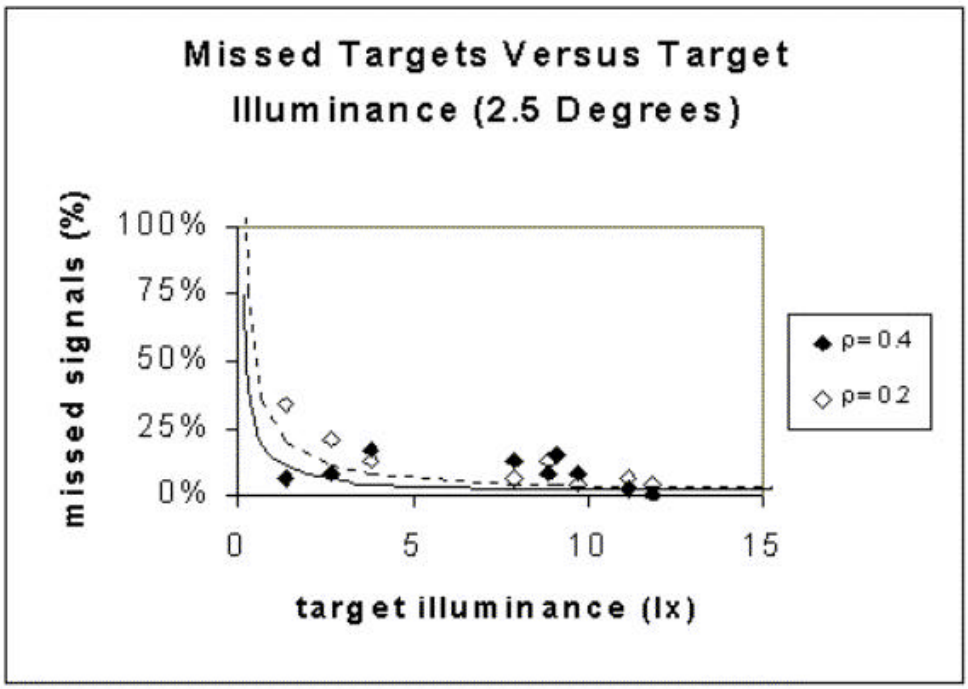

FIGURE 7 Missed target percentages for targets located 7.5° from the line of sight.

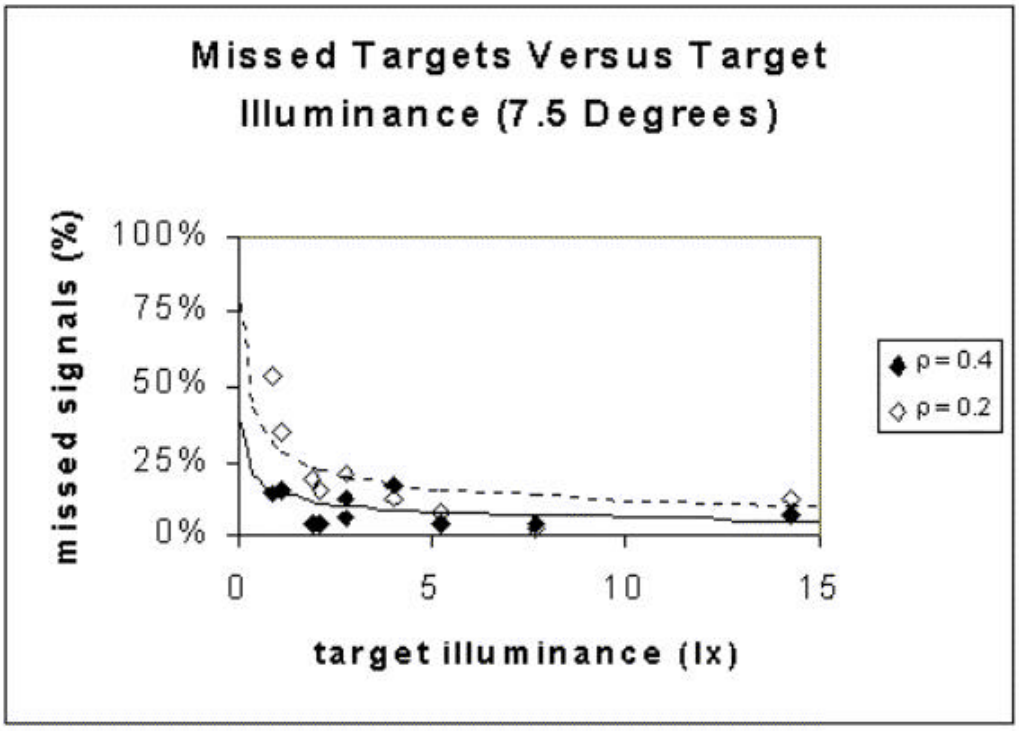

FIGURE 8 Missed target percentages for targets located 12.5° from the line of sight.

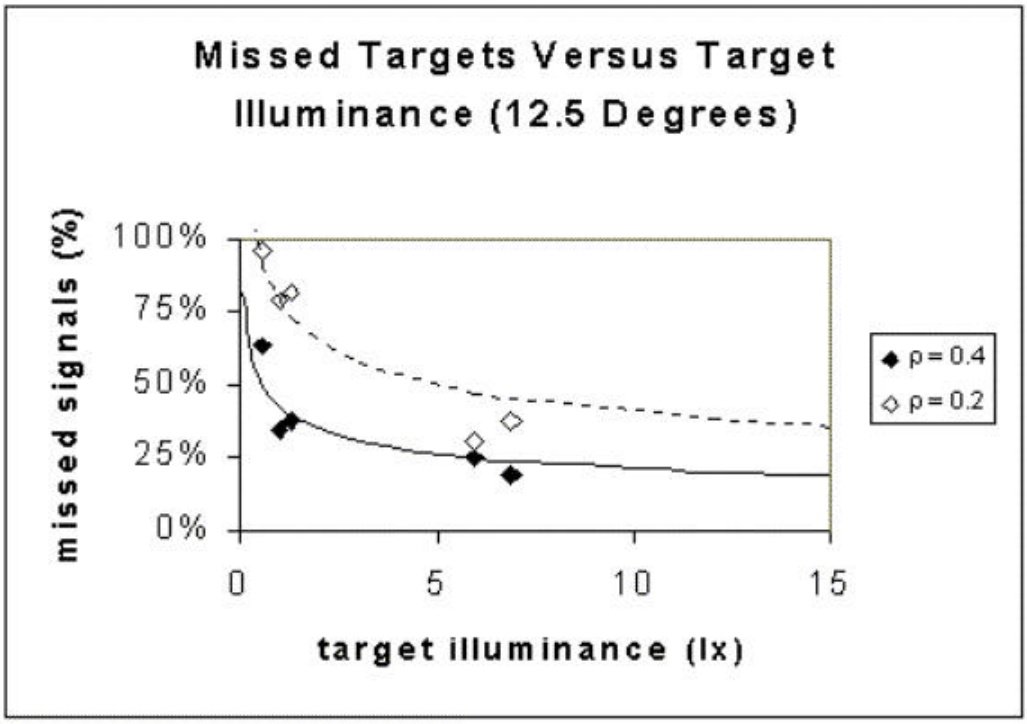

FIGURE 9 Missed target percentages for targets located 17.5° from the line of sight.

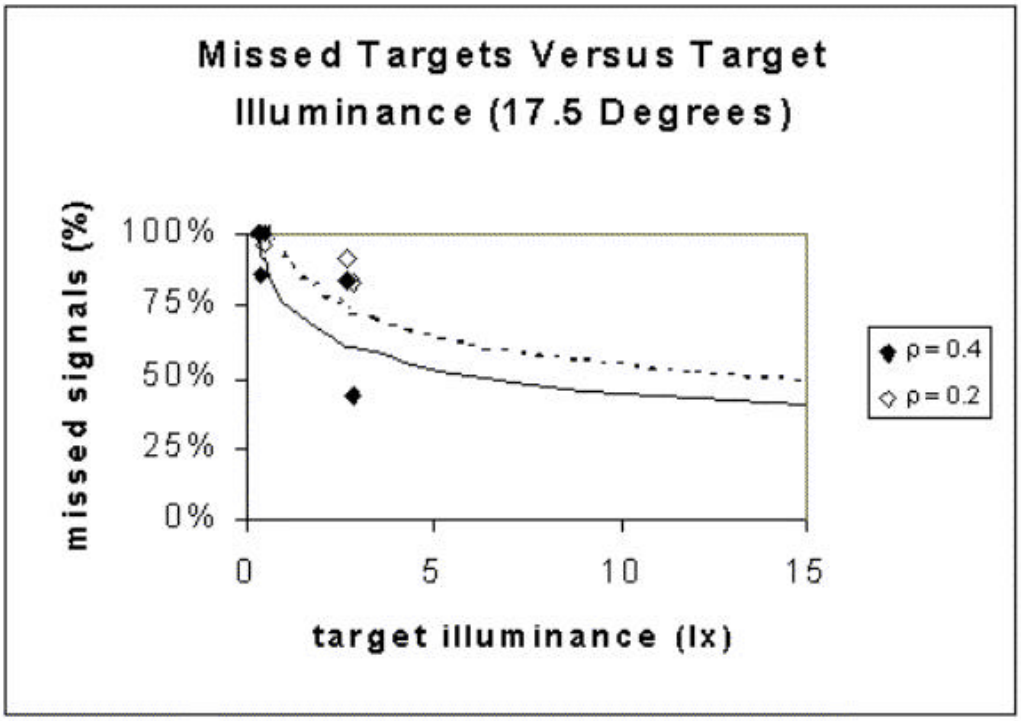

FIGURE 10 Best fitting values of *a* in the model $RT = aE^{-0.33} + n$, where n = 400 ms, for each target reflectance.

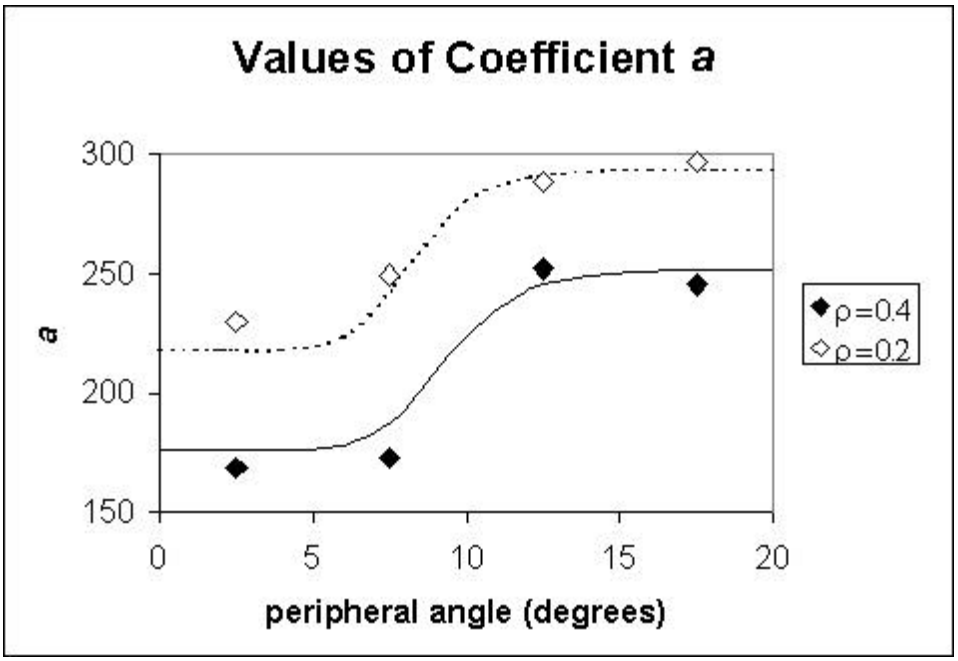

FIGURE 11 Best fitting values of *b* as a function of reflectance, for the expression $a = b - (b - c)/(1 + (\rho/d)^e)$.

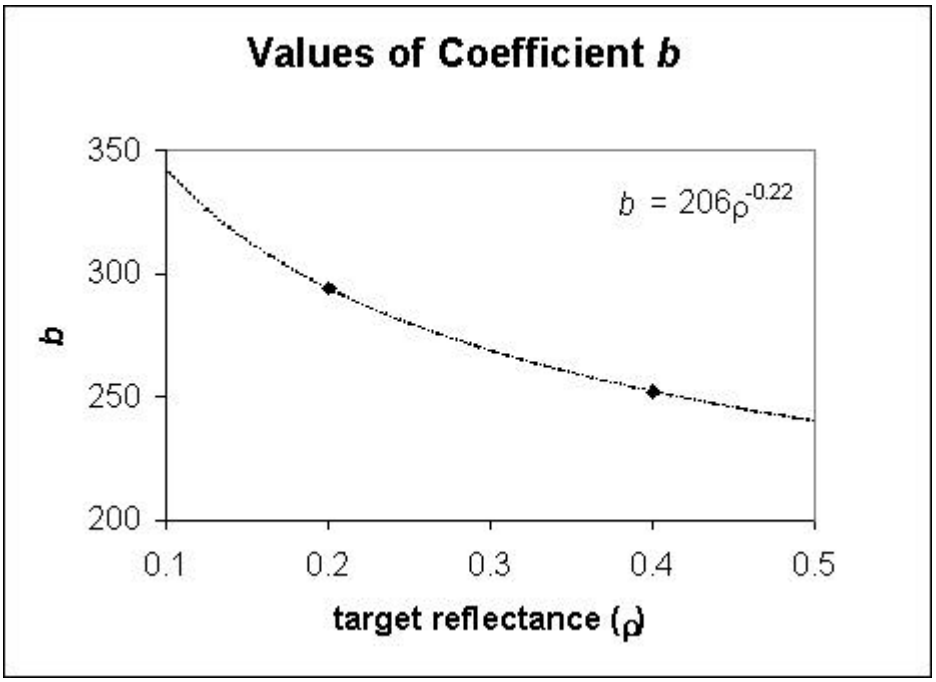

FIGURE 12 Best fitting values of *d* as a function of reflectance, for the expression $a = b - (b - c)/(1 + (\rho/d)^e)$.

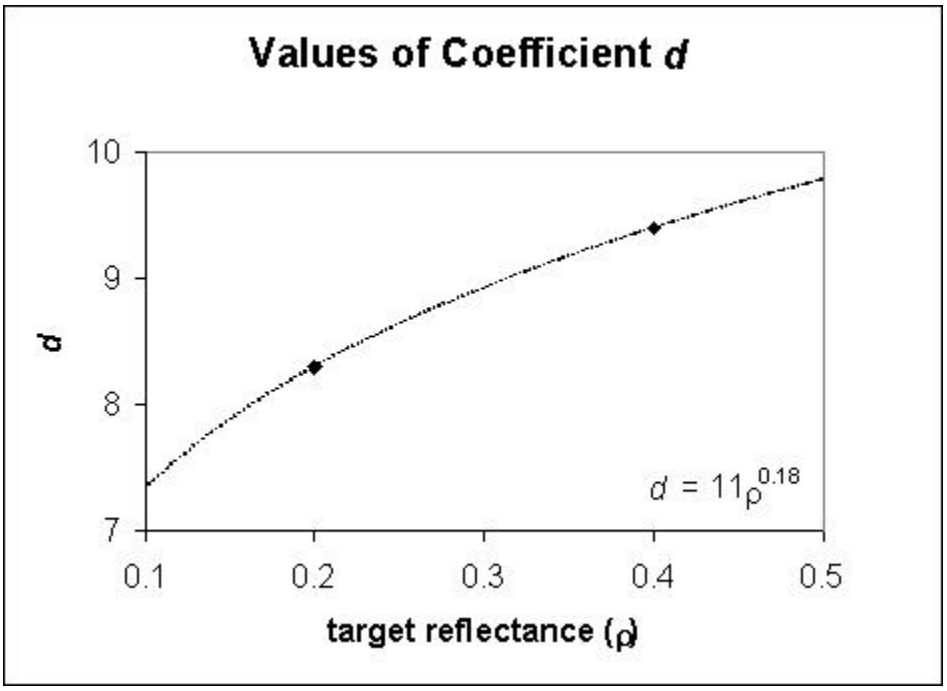

FIGURE 13 Best fitting values of *f* in the model $MT = fE^{-g}$, for each target reflectance.

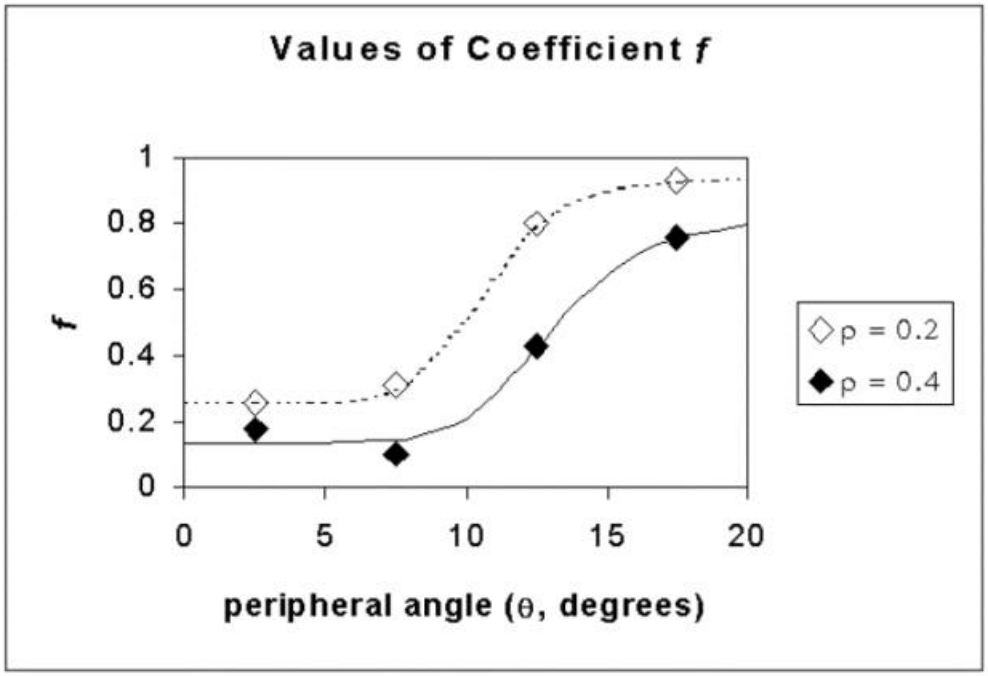

FIGURE 14 Best fitting values of *g* as a function of target angle, for the expression $MT = fE^{-g}$.

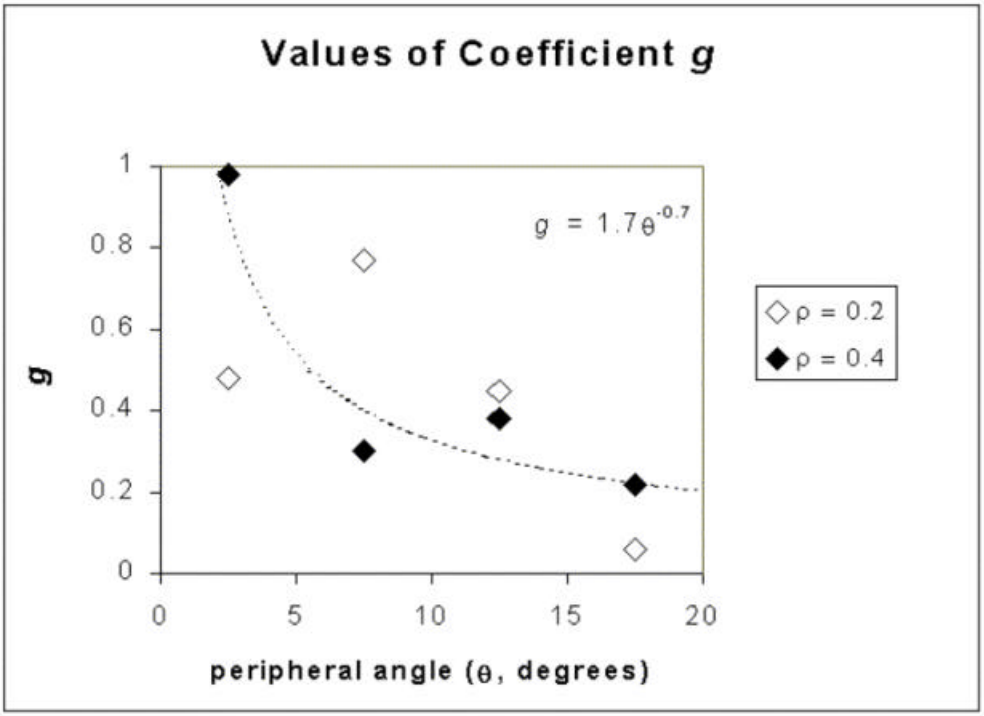

FIGURE 15 Best fitting values of *h* as a function of reflectance, for the expression $f = h - (h - k)/(1 + (q/k)^m)$.

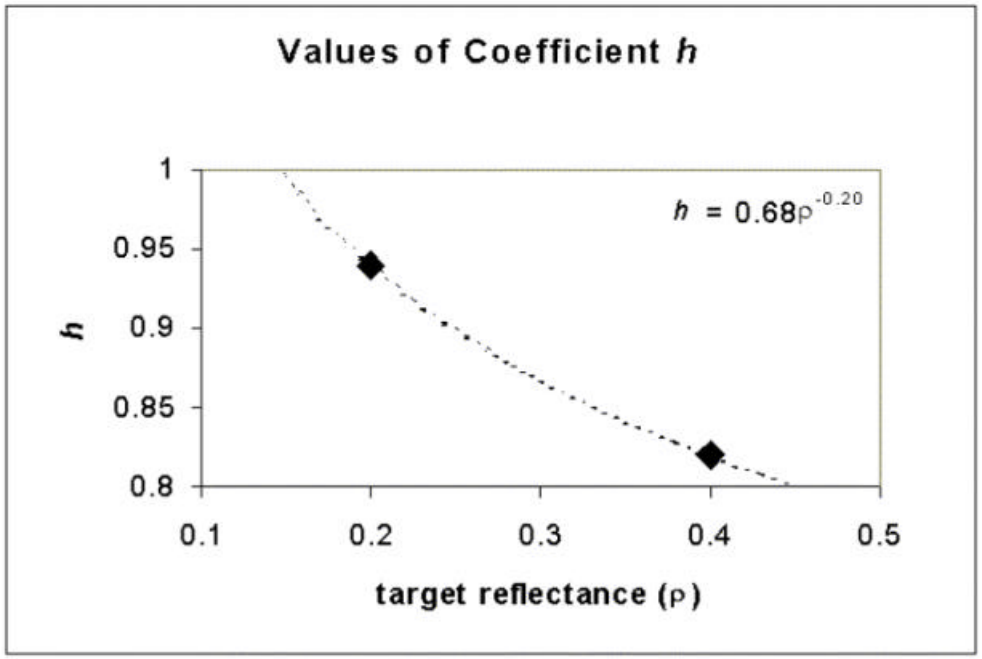

FIGURE 16 Best fitting values of *k* as a function of reflectance, for the expression $f = h - (h - k)/(1 + (q/k)^m)$.

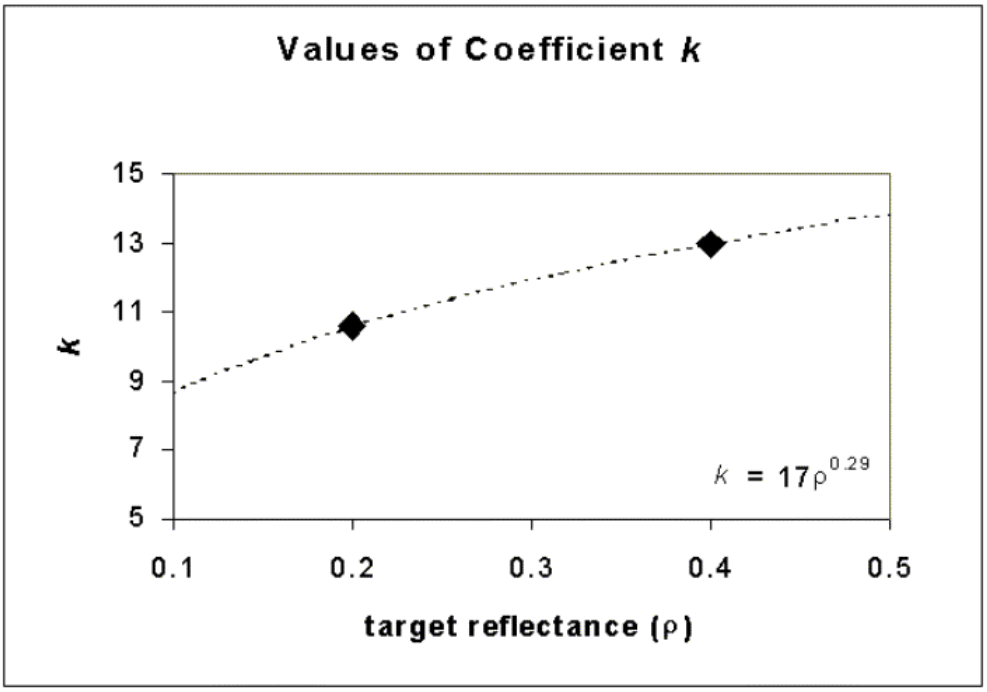

FIGURE 17 Surface plots showing the impact of target reflectance and location on predicted reaction times for four headlamp illuminances.

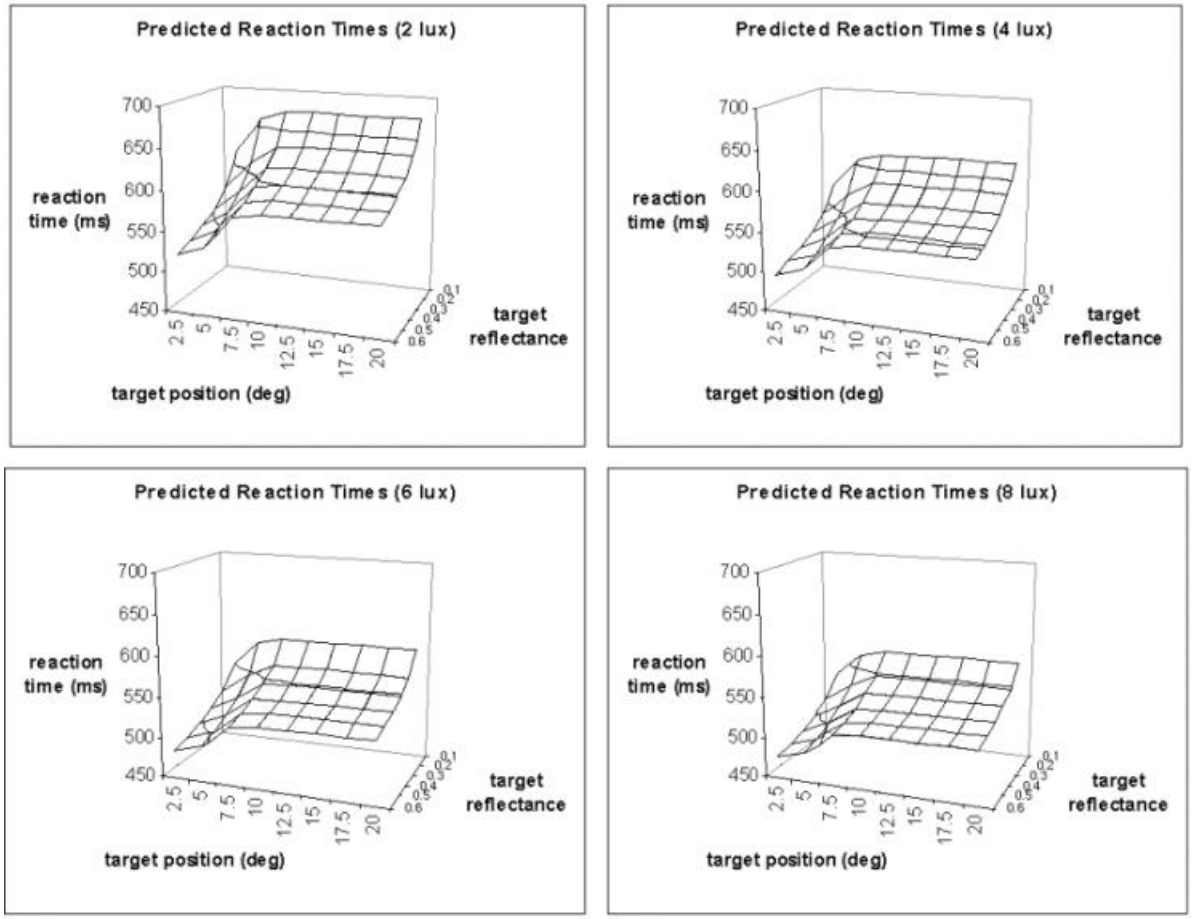

FIGURE 18 Surface plots showing the impact of target reflectance and location on predictions of missed targets for four headlamp illuminances.